BBA - General Subjects 1864 (2020) 129484

Contents lists available at ScienceDirect

BBA - General Subjects

journal homepage: www.elsevier.com/locate/bbagen

Metabolic fingerprinting reveals extensive consequences of GLS hyperactivity

Lynne Rumping[a,b,c], Mia L. Pras-Raves[a,b], Johan Gerrits[a], Yuen Fung Tang[a], Marcel A. Willemsen[a,b], Roderick H.J. Houwen[c], Gijs van Haaften[a,b], Peter M. van Hasselt[c], Nanda M. Verhoeven-Duif[a,b], Judith J.M. Jans[a,b,*]

[a] Department of Genetics, University Medical Center Utrecht, Utrecht University, Utrecht, 3584, CX, the Netherlands
[b] Center for Molecular Medicine, University Medical Center Utrecht, Utrecht University, Utrecht, 3584, CX, the Netherlands
[c] Department of Pediatrics, University Medical Center Utrecht, Utrecht University, Utrecht, 3584, CX, the Netherlands

ARTICLE INFO

Keywords:
DI-HRMS
Untargeted metabolomics
Metabolic profiling
Glutaminase activity
Glutamate metabolism

ABSTRACT

Background: High glutaminase (GLS;EC3.5.1.2) activity is an important pathophysiological phenomenon in tumorigenesis and metabolic disease. Insight into the metabolic consequences of high GLS activity contributes to the understanding of the pathophysiology of both oncogenic pathways and inborn errors of glutamate metabolism. Glutaminase catalyzes the conversion of glutamine into glutamate, thereby interconnecting many metabolic pathways.

Methods: We developed a HEK293-based cell-model that enables tuning of GLS activity by combining the expression of a hypermorphic GLS variant with incremental GLS inhibition. The metabolic consequences of increasing GLS activity were studied by metabolic profiling using Direct-Infusion High-Resolution Mass-Spectrometry (DI-HRMS).

Results and conclusions: Of 12,437 detected features [*m/z*], 109 features corresponding to endogenously relevant metabolites were significantly affected by high GLS activity. As expected, these included strongly decreased glutamine and increased glutamate levels. Additionally, increased levels of tricarboxylic acid (TCA) intermediates with a truncation of the TCA cycle at the level of citrate were detected as well as increased metabolites of transamination reactions, proline and ornithine synthesis and GABA metabolism. Levels of asparagine and nucleotide metabolites showed the same dependence on GLS activity as glutamine. Of the nucleotides, especially metabolites of the pyrimidine thymine metabolism were negatively impacted by high GLS activity, which is remarkable since their synthesis depend both on aspartate (product of glutamate) and glutamine levels. Metabolites of the glutathione synthesizing γ-glutamyl-cycle were either decreased or unaffected.

General significance: By providing a metabolic fingerprint of increasing GLS activity, this study shows the large impact of high glutaminase activity on the cellular metabolome.

Synopsis

Glutaminase interconnects a multitude of metabolic pathways. This study shows the metabolic responses to high GLS activity as revealed by metabolic profiling.

- Expression of a hypermorphic *GLS* variant in combination with incremental GLS inhibition enables tuning of GLS activity.
- DI-HRMS provides an in-depth metabolic fingerprint recapitulating metabolic consequences of in vivo enhanced GLS activity.
- High GLS activity solely is sufficient to cause a truncated TCA cycle.
- High GLS activity may negatively impact pyrimidine metabolism.

1. Introduction

Inborn errors of metabolism are often the consequence of disturbed enzyme activity secondary to genetic alterations. Insight into the effect of the genetic alteration on enzyme activity can be gained by determining levels of the substrate, product and closely related metabolites. The study of more extensive downstream metabolic consequences of disturbed enzyme activity might create additional insight into the

* Corresponding author at: Department of Genetics, University Medical Center Utrecht, Utrecht University, Utrecht, 3584, CX, the Netherlands
E-mail address: j.j.m.jans@umcutrecht.nl (J.J.M. Jans).

https://doi.org/10.1016/j.bbagen.2019.129484
Received 15 May 2019; Received in revised form 1 November 2019; Accepted 4 November 2019
Available online 14 November 2019

pathophysiological mechanism of disease. Untargeted metabolomics

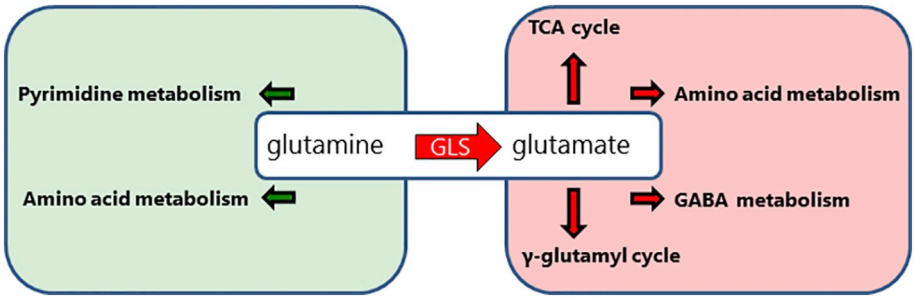

using Direct-Infusion High-Resolution Mass Spectrometry (DI-HRMS) provides a metabolic fingerprint, enabling the investigation of alterations in the metabolome induced by pathogenic stimuli and genetic alterations.

Altered glutaminase (GLS; l-glutaminase, EC 3.5.1.2) activity is an important pathophysiological phenomenon in tumorigenesis and in two genetic metabolic diseases. GLS catalyzes the conversion of glutamine into glutamate, two amino acids at the center of a multitude of metabolic pathways [1]. Glutamate can be converted into the TCA-cycle intermediate α-ketoglutarate by transamination, with concomitant production of amino acids which are used for protein and nucleotide synthesis [2]. In parallel, glutamate is the precursor of the neurotransmitter GABA, glutamic-γ-semialdehyde -intermediates in proline and ornithine synthesis- and of the anti-oxidant glutathione. Glutamine on the other hand is important for asparagine synthesis as well as for nucleotide synthesis [2–4]. GLS is strictly regulated under physiological conditions, suggesting that derangements are disadvantageous [5,6]. Given the divergent roles of both glutamine and glutamate, the consequences of changes in GLS activity on the involved processes cannot easily be predicted. It is therefore difficult to assess which metabolic consequences are responsible for a phenotypic outcome, and therefore to determine a potential therapeutic target. The detrimental consequences of increased GLS activity are illustrated by the recently described inborn error of metabolism in which GLS hyperactivity due to a hypermorphic germline variant leads to glutamate excess in a child with infantile cataract and developmental delay [6]. These phenotypic features are assumed to be the direct consequence of glutamate excess and –more downstream- of oxidative stress. However, other downstream consequences might also contribute to the pathophysiology. In numerous tumor types GLS overexpression appears to favor tumorigenesis or tumor progression. Increased presence of glutamate fuels the TCA cycle and provides the cell with building blocks, such as amino acids and nucleotides as well as the antioxidant glutathione [3,4,7]. Based on these observations, GLS inhibition is currently tested in clinical oncology to halt tumor growth [8]. GLS overexpression in this context, however, is usually due to oncogenic c-Myc, c-Jun and Sirtuins, which regulate the expression of GLS together with many other genes, thus precluding a definite conclusion of the role of GLS [9,27,28].

In this study, we developed a model that allows the delineation of the metabolic consequences of high GLS activity. The model is based on the expression of the recently described hypermorphic *GLS* germline variant (*GLS* p.Ser482Cys) followed by incremental GLS inhibition, enabling tuning of GLS activity [6]. DI-HRMS provided an in-depth metabolic fingerprint, capturing the extensive metabolic consequences of increasing GLS activity. This study creates insight into the metabolic consequences of high GLS activity and contributes to the understanding of the pathophysiology of both oncogenic pathways and inborn errors of glutamate metabolism.

2. Results and discussion

2.1. Modeling high GLS activity

To generate a cell model expressing high GLS activity, HEK293 cells were stably transfected with the *GLS* p.Ser482Cys hyperactivity variant [6]. This hypermorphic variant causes intrinsically increased GLS activity rather than GLS overexpression. As expected, UPLC-MS/MS amino acid analysis revealed increased intracellular glutamate concentrations and decreased glutamine concentrations compared to cells transfected with an empty vector, indicating successful transfection and high GLS activity. It should be kept in mind that ammonia-induced glutamate oxidation might also have influenced glutamine and glutamate levels [29]. Stepwise inhibition of GLS activity down to baseline activity was obtained by adding CB-839 at increasing concentrations. Exposing cells to 10 μM completely normalized glutamine and glutamate concentrations (Fig. 1A, Fig. S1). CB-839 is a specific allosteric inhibitor and off-targets effects are not expected [8]. Although CB-839 has low nanomolar potency against GLS in most cell lines, there is a clear dose effect of CB-839, which can probably be explained by the extremely high GLS activity caused by the hypermorphic variant [6]. This model thus enables tuning of GLS activity and thereby provides a powerful tool to dissect the metabolic consequences of isolated GLS overactivity.

2.2. DI-HRMS

DI-HRMS analysis of cellular extracts with varying GLS activity levels led to the detection of 12,437 features [m/z] (Table S2). 109 features with an accurate mass corresponding to endogenous metabolites based on the Human Metabolome Database were significantly altered upon high GLS activity ($p < .05$ with t-test and $R^2 > 0.6$ on linear regression) (Table S3). Among these metabolites were glutamate and glutamine. The intensities of glutamate and glutamine, both the individual and sum of the adducts, obtained by untargeted DI-HRMS corresponded well with the concentrations obtained by targeted UPLC-MS/MS (Fig. 1B, Table 1).

2.3. Metabolic consequences of high GLS activity

As expected, metabolic profiling revealed that high GLS activity increases the concentration of multiple metabolites downstream from glutamate while decreasing the concentration of metabolites downstream of glutamine as compared to normal GLS activity (Fig. 2, Table 1).

Specifically, high GLS activity led to increased levels of α-ketoglutarate -the direct product of glutamate transamination- as well as the TCA cycle intermediates succinate, fumarate, malate and oxaloacetate.

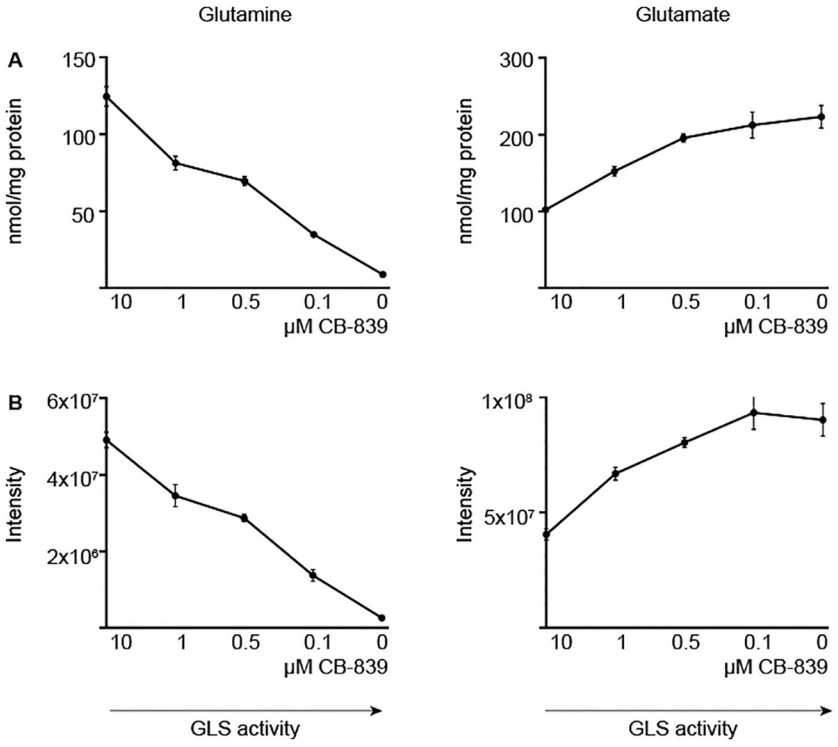

Fig. 1. Glutamine and glutamate levels in HEK293 cells stably transfected with a hypermorphic GLS variant, in which GLS is stepwise inhibited with CB-839. A. Targeted analyses by UPLC-MS/MS show that inhibition of GLS results in increased glutamine and decreased glutamate concentrations. Data represents mean concentrations of biological triplicates corrected for protein ($n = 3$) with standard deviations. B. The same pattern of these amino acids was detected by untargeted metabolomics using DI-HRMS. Data represent the mean intensities in biological triplicates of the sum of adducts (positive mode, negative mode, Na^+, K^+, Cl^-) with standard deviations.

Table 1
Detected metabolites sorted by metabolic pathway. Metabolites without adducts measured in positive (+) or negative (−) mode, or with adducts (K^+ Na^+ Cl^-) sorted by metabolic pathways. Metabolites involved in multiple pathways are listed only ones. The R^2 and *p*-value of only the metabolite-adduct with the highest R^2 is shown. ↓ decreased; ↑ increased; = not affected ($R^2 < 0.6$ or $p > .05$). Metabolites with the same mass are displayed in the same cell or symbolized with Δ * O.

Pathway	Compound	HMDB-code	Adducts	Slope	R2	p-value
GLS reaction	Glutamine$^{\Delta}$	HMDB00641	K^+ Na^+ Cl^- + −	↓	0.99	3.63 E-07
	Glutamate*	HMDB00148	K^+ Na^+ Cl^- + −	↑	0.88	8.21 E-05
TCA cycle	α-Ketoglutarate	HMDB00208	−	↑	0.73	4.38 E-04
	Succinate	HMDB00254	Na^+	↑	0.69	2.43 E-02
	Fumarate	HMDB00134	Cl^- −	↑	0.84	1.00 E-06
	Malate	HMDB00156	Na^+ +	↑	0.72	4.21 E-05
	Oxaloacetate	HMDB00223	Cl^-	↑	0.73	2.01 E-02
	Cis-aconitate	HMDB00072	−	↓	0.64	7.53 E-04
	Citrate	HMDB00094	−	↓	0.62	1.07 E-04
	Iso-citrate	HMDB00193				
	Alanine	HMDB00161	+ −	↑	0.84	4.16 E-03
Serine glycine metabolism	Phosphohydroxypyruvate	HMDB01024	Na^+	↑	0.68	8.15 E-03
	Phosphoserine*	HMDB00272	K^+ Na^+ Cl^- + −	↑	0.88	3.08 E-04
	Serine	HMDB00187	K^+	↑	0.74	1.54 E-03
	Glycine	HMDB00123	+ −	=	0.12	0.62
GABA metabolism	GABA^{o}	HMDB00112	−	↑	0.85	3.96 E-05
	Succinate-semialdehyde	HMDB01259	−	↑	0.66	2.48 E-03
Proline - ornithine – glutathione metabolism	Glutamic-γ-semialdehyde	HMDB02104	K^+	↑	0.63	2.00 E-03
	1-Pyrroline-5-carboxylate	HMDB01369	+	↑	0.78	8.08 E-04
	Ornithine	HMDB00214	Na^+	↑	0.68	2.37 E-02
	γ-Glutamyl-alanine	HMDB06248	K^+ Na^+ Cl^- −	↓	0.90	1.13 E-05
	γ-Glutamyl-glutamine	HMDB29147	− +	↓	0.73	3.12 E-07
	γ-Glutamyl-analyl-glycine	HMDB05766				
	5-Oxoproline	HMDB00267	+	↓	0.63	6.11 E-03
	Reduced glutathion	HMDB00125	+ −	=	0.17	0.07
Asparagine metabolism	Asparagine	HMDB00168	Cl^- −	↓	0.84	6.66 E-07
	Aspartate	HMDB00191	K^+ Na^+ Cl^- + −	↑	0.96	2.94 E-06
Nucleotide metabolism	Thymine	HMDB00262	−	↓	0.79	4.18 E-03
	Dihydrothymine	HMDB00079	K^+ Na^+ −	↓	0.98	4.65 E-06
	Deoxycytidine	HMDB00014	+	↓	0.64	8.94 E-03
	Ureido-isobutyrate$^{\Delta}$	HMDB00641	K^+ Na^+ Cl^- + −	↓	0.99	3.63 E-07
	3-Amino-isobutyrate^{o}	HMDB00112	−	↑	0.85	3.96 E-05
	Urate	HMDB00289	+	↓	0.89	9.48 E-04
	Dihydrouracil	HMDB00076	−	↓	0.82	2.94 E-05
	Xanthosine triphosphate	HMDB00293	+	↑	0.64	4.29 E-02
	Deoxyinosine	HMDB00071	–	↓	0.63	1.08 E-02

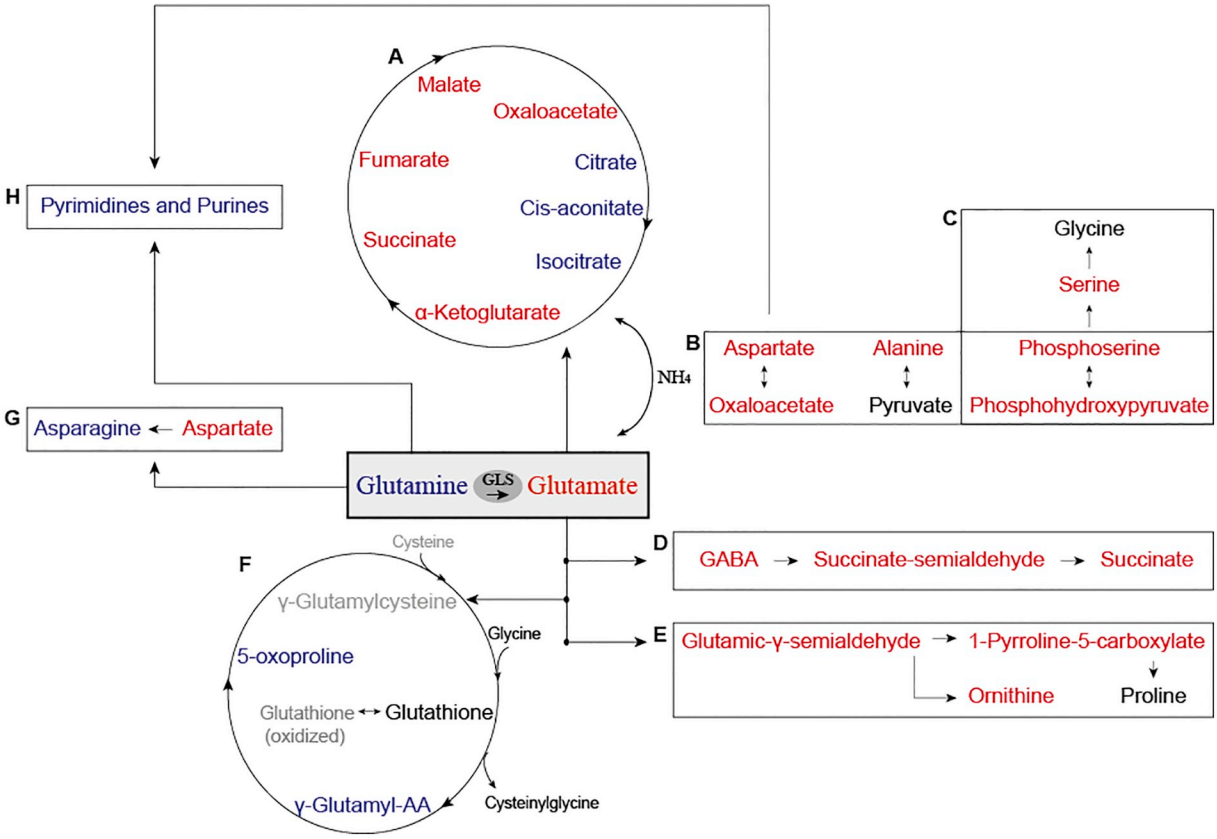

Fig. 2. Metabolic pathways interconnected by GLS and their response to high GLS activity. DI-HRMS detected increased (red), decreased (blue) or non-affected (black) metabolites upon high GLS activity. Undetected metabolites (non-informative) are marked in grey. A. TCA cycle via α-ketoglutarate produced by dehydrogenation or transamination of glutamate. B. Transamination reactions coupled to the reversible conversion of glutamate into α-ketoglutarate. C. Serine and glycine biosynthesis from phosphoserine, produced by transamination. D. GABA, a direct product of glutamate decarboxylation. E. Proline and ornithine biosynthesis from glutamic-γ-semialdehyde. F. γ-glutamyl cycle metabolizes glutathione from glutamate, glycine and cysteine. G. Asparagine synthesis from aspartate, requiring nitrogen from glutamine. H. Purine and pyrimidine synthesis, requiring both glutamine and aspartate.

Levels of cis-aconitate, and citrate and/or isocitrate were decreased. This combination of alterations is known as a truncated TCA cycle (Figs. 2A, 3, Table 1) [10]. As citrate and isocitrate share the same mass and therefore cannot be distinguished by DI-HRMS, we validated these findings by UPLC-MS/MS and confirmed these results (Fig. S2). There are several possible explanations for the truncation of the TCA cycle: i.e. effected gluconeogenesis/glycolysis causing decreased acetyl-CoA levels; increased ROS-levels interrupting citrate metabolism and an outflow of oxaloacetate by transamination into aspartate [10]. The truncated TCA cycle as a result of increased glutaminolysis has been described in glutamine-dependent cancer cells. In these cancer cells, GLS expression is upregulated in parallel to other c-Myc, C-Jun and Sirtuins induced alterations, supporting tumorigenesis and tumor progression [7,11] [27,28]. Our results show that high GLS activity solely is sufficient to drive this phenomenon.

Transamination of glutamate into α-ketoglutarate is coupled to the production of amino acids - particularly aspartate, alanine and phosphoserine- from organic acids. The levels of these amino acids increased upon high GLS activity, suggesting that high GLS activity leads to an increased transamination rate and amino acid production (Fig. 2B). Serine levels also increased, most likely following from increased phosphoserine levels (Fig. 2C). The level of glycine, which is one enzymatic step more distant from GLS, was unaffected by GLS activity. In addition to increased levels of transamination products and GABA -a direct product of glutamate conversion by glutamate decarboxylase- and its breakdown products succinate-semialdehyde and succinate increased with high GLS activity (Fig. 2D).

Proline and ornithine are produced from glutamate through glutamic-γ-semialdehyde and pyrroline-carboxylate. Glutamic-γ-semialdehyde, pyrroline-carboxylate and ornithine were increased at high GLS activity (Fig. 2E). The level of proline -one step more distant from GLS- was unaffected.

GLS activity is considered the drive for glutathione synthesis through the γ-glutamyl-cycle. Surprisingly, metabolites of the γ-glutamyl-cycle, rather than increased, were either decreased (γ-glutamyl-alanine, γ-glutamyl-glutamine and/or γ-glutamyl-analyl-glycine and oxoproline) or unaffected (glycine, cysteinylglycine, reduced glutathione). As the γ-glutamyl-cycle produces the anti-oxidant glutathione, this appears to be in contrast with reports of cancer cells with upregulated GLS expression in which glutathione synthesis was found to be increased [4]. We previously observed that GLS hyperactivity decreases redox buffering capacity, probably secondary to glutamate excitotoxicity [6,12]. Our finding suggests that increased glutathione synthesis in cancer cells may be caused by the induction of additional enzymes and of glutamate-cysteine transporter expression, rather than induction of GLS alone [26].

In line with a glutamine decrease, high GLS activity resulted in a decrease of asparagine, which is produced by nitrogen transfer from glutamine to aspartate (Fig. 2G). Interestingly, the biosynthesis of pyrimidine and purine nucleotides requires both glutamine and aspartate and is therefore linked to both sides of the GLS reaction (Fig. 2H) [2]. We show that high GLS activity leads to decreased levels of the pyrimidine thymine and its degradation products dihydrothymine, deoxycytidine and possibly ureido-isobutyrate. Next to thymine metabolism, the purine urate and other related metabolites were affected, but these did not explicitly point towards a single pathway (Table 1).

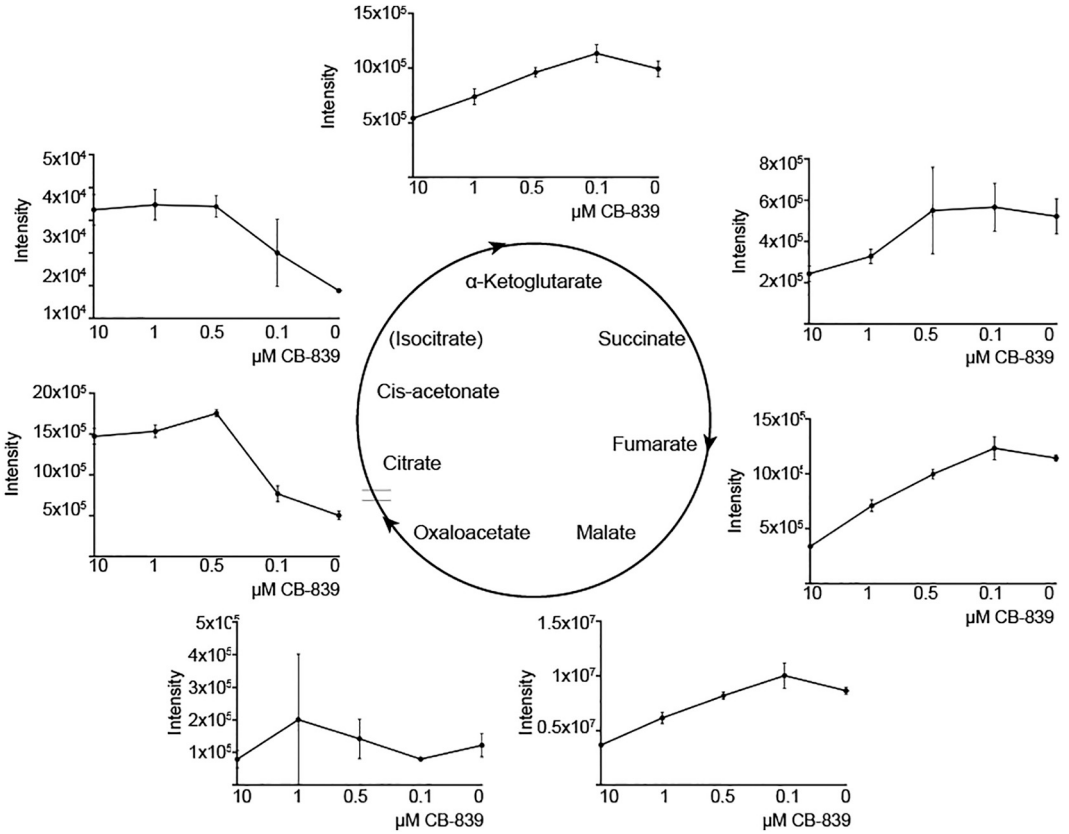

Fig. 3. High GLS activity leads to a fueled, truncated TCA cycle. DI-HRMS reveals increased adduct ions of α-ketoglutarate, succinate, fumarate, malate and oxaloacetate and decreased cis-aconitate, isocitrate and/or citrate (same *m/z*, therefore presented only once) levels upon high GLS activity. Affected metabolites were defined based on individual adduct ions (Table 1), Data presented here show the sum of the intensities of all adduct ions (affected and unaffected). Measurements are performed in biological and technical replicates with standard deviations.

These results indicate that high GLS activity decreases the synthesis of thymine and possibly of nucleotides in general by depriving cells from glutamine, an effect that could be alleviated by GLS inhibition. This notion contrasts previous reports which concluded that GLS upregulation in cancer cells favors nucleotide synthesis -and thereby tumor growth- by providing these cells with glutamate-derived aspartate [3,14]. This disparity underlines the necessity of both glutamine and aspartate availability for nucleotide synthesis. Although this discrepancy may reflect a cell type-specific response to pathophysiological stimuli due to the unique metabolic composition of each cell type, it also suggests that the increased nucleotide synthesis in cancer cells with upregulated GLS activity is not caused by enhanced glutaminolysis, but rather by other c-Myc, c-Jun and Sirtuins related changes. In addition to differential GLS isoform expression in different cancer types, this may explain why GLS inhibition has different therapeutic effects in different cancer cells while in all of these cancers GLS expression is upregulated [15]. We show that GLS inhibition restores glutamine levels, which may -undesirably- favor nucleotide synthesis. This implies that GLS inhibition as a therapeutic treatment should be carefully considered per tumor type.

In addition to the pathways directly linked to GLS, 54 other features (*m/z*) were affected (Table S3). Among these were several increased metabolites of gluconeogenesis or glycolysis (phosphoenolpyruvate, 2-phosphoglycerate and/or 3-phosphoglycerate, fructose-6-phosphate and/or glucose-6-phosphate). Other affected metabolites include the carnitines acetylcarnitine, propionylcarnitine, butyrylcarnitine and/or isobutyrylcarnitine, which decreased with high GLS activity. These metabolites are not evidently or directly related to glutamine or glutamate. They underscore the extensiveness of metabolic changes upon a single enzymatic alteration and have the potential to unveil novel metabolic connections.

This study creates insight into the pathophysiology of the *GLS* germline hyperactivity mutation found in an infant with cataract and profound developmental delay [6]. The clinical features are assumed to be the direct cause of a neurotransmitter imbalance and of oxidative stress secondary to glutamate excess, as increased glutamate was shown to decrease redox buffer capacity. This is supported by our findings of decreased γ-glutamyl-cycle metabolites. Furthermore, both the neurotransmitters glutamate and GABA levels were increased. If this reflects the situation in the brain in vivo, this imbalance might also contribute to the profound developmental delay. Additionally, defects in purine and pyrimidine regulation are associated with neurodevelopmental defects [16]. These metabolic consequence of GLS hyperactivity are interesting leads that help uncover the pathophysiology of this novel inborn error of metabolism (IEM). Recently, another IEM involving GLS caused by germline *GLS* loss-of-function mutations has been described. These patients have a phenotypic spectrum ranging from optic atrophy to fatal, neonatal encephalopathy, without a clear pathophysiological mechanism [17,18,30]. Metabolic profiling of the consequences of these *GLS* loss-of-function mutations by DI-HRMS might provide interesting leads towards the pathophysiology.

Metabolic fingerprinting by DI-HRMS generates an overview of many metabolic pathways and their changes upon pathogenic stimuli or genetic alterations. It should be noted, however, that the metabolic profile obtained in this study reflects a cell type-specific response to pathophysiological stimuli. The unique metabolic composition of each cell-type -and organ impedes the translation of these results towards other cell-types. Of importance, DI-HRMS detects masses (*m/z*) that may not be unique to one metabolite. Since multiple metabolites may share the same molecular mass, the identification of these metabolites

is limited using DI-HRMS, requiring validation of findings by targeted analyses to confirm and further explore interesting leads, as was done in this study for the TCA intermediates.

Taken together, by combining a cell model that allows tuning of GLS activity with DI-HRMS, we were able to study the metabolic responses directly related to high GLS activity in a HEK293 cell model.

3. Material and methods

3.1. Cell culture and sample preparation

A cell line with GLS hyperactivity was created by stably transfecting HEK293 T-REx Flp-in host cell lines with a plasmid containing KGA (the long splice variant of *GLS*) with the Ser482Cys mutation known to lead GLS hyperactivity, as previously described by Rumping et al. [6]. For plasmid preparation, the Ser482Cys cDNA sequence was obtained by site-specific mutagenesis (QuikChange II XL, Agilent, Santa Clara, CA, USA) of the wildtype KGA sequence in pcDNA5/FRT/TO TOPO containing a hybrid CMV/TetO_2 promoter for regulated expression (Life Technologies, Waltham, MA, USA). Cells were cultured at 37 °C in 5% CO_2 in DMEM-GlutaMax high glucose with pyruvate. Medium was supplemented with 200 μg/ml hygromycine (Roche, Mannheim, Germany) for selection of plasmid-containing HEK293 cells and with 10% heat-inactivated fetal bovine serum, 100 U/ml penicillin, 0.1 mg/ml streptomycin and 2 mM L-glutamine (obtained from Gibco by Life Technologies, Waltham, MA, USA, unless stated differently). Cells were frequently tested for mycoplasma.

The GLS vector was induced with 0.1 μg/ml tetracycline. Simultaneously, the cells were incubated with 0 μM, 0.1 μM, 0.5 μM, 1 μM and 10 μM CB-839 (Selleckchem, Houston, USA) for 15 h to obtain different levels of GLS activity [19]. Cells were collected in methanol (Sigma-Aldrich, Steinheim, Germany) -of which supernatants were evaporated with nitrogen and reconstituted in 1 ml of methanol for metabolomics or in lysis buffer for protein quantification. Lysis buffer containing 1% Triton X-100 (Sigma-Aldrich, Steinheim, Germany), 50 mM Tris (Roche, Mannheim, Germany), 150 mM NaCl and protease inhibitor (Roche, Mannheim, Germany) was used. Protein quantification was performed using the Pierce BSA assay kit (Thermo Fisher Scientific, Waltham, MA, USA) in biological and analytical triplicates.

3.2. Untargeted metabolomics

3.2.1. Direct-infusion high-resolution mass spectrometry (DI-HRMS)

Direct infusion was performed on the TriVersa NanoMate (Advion, Ithaca, NY, USA) using chip-based infusion (400 nozzles, nominal internal Ø 5 μm). High-resolution mass spectrometry (140.000 at *m/z* 200 Da) was performed with a Q-ExactivePlus (Thermo Scientific GmbH, Bremen, Germany) in a scan range of *m/z* 70 to 600 in negative and positive modes [20]. Each condition was performed in biological triplicates and each sample was measured in technical triplicate to improve the accuracy of observed intensities. To achieve high mass accuracy, mass calibration of the instrument was performed and internal lock masses were used [21].

3.2.2. Pipeline

RAW data files were converted to mzXML format using MSConvert [22]. The data were processed using an in-house developed untargeted metabolomics pipeline written in the R programming language. First, the mzXML files were converted to readable format by the XCMS package [23]. For every sample, peak finding was done by fitting Gaussian-shaped curves over the data on the *m/z* axis. Peaks with the same m/z (within 2 ppm) were grouped over different samples. Peak groups were identified using all entries in the Human Metabolome DataBase (HMDB) and isotopes, using an accuracy of 3 ppm or better and those with intensities > 5000 in all technical triplicates of at least one biological sample were included [24]. The intensities of the technical replicates were averaged. The statistical analysis was a linear regression of measured intensities on the ordinal concentrations (i.e. 10, 1, 0.5, 0.1 and 0 μM were represented as ordinal values 1 through 5).

3.2.3. Selection of metabolites

A selection of metabolites without adducts or with the adducts Na^+, K^+ or Cl^- of endogenous origin according to the HMDB was made. A linear curve of the average intensity of 9 replicates (technical triplicates for every biological replicate) against several GLS activity levels -achieved by different CB-839 concentrations- was plotted. Statistical analyses were performed by the calculation of the R^2 on a linear regression of the curve and a *t*-test on the extremities. Those metabolites with $R^2 > 0.6$ and $p < .05$ were considered affected and included in further analyses.

3.3. Targeted metabolomics

3.3.1. Glutamine and glutamate

The concentrations of these amino acids were determined by UPLC-MS/MS using stable isotope-labeled internal standards as previously described [25].

3.3.2. TCA cycle intermediates

3.3.2.1. Chromatographic separation. Sample analysis was performed on a Waters Acquity™ ultraperformance liquid chromatography (UPLC) system Waters Corp., Milford, USA). Chromatographic separation was performed at 30 °C using an Acquity HSS T3 column (100 mm × 2.1 mm i.d., 1.8 μm; Waters Corp., Milford, USA) equipped with an ACQUITY UPLC VanGuard Pre-Column HSS T3 (5 mm × 2.1 mm i.d., 1.8 μm). The following eluents were used: solvent A: H_2O, 0.1% (formic acid) (*v*/v); solvent B: 100% acetonitrile. The gradient elution was as follows: 0–4.0 min isocratic 1% B, 4.0–4.5 min linear from 1% to 100% B, 4.5–5.0 min isocratic 100% B, and 5.0–5.1 min linear from 100% to 1% B, with 5.1–6.0 min for initial conditions of 1% B for column equilibration. The flow rate remained constant at 0.3 ml/min. 10 μl injection volume was used.

3.3.2.2. Standard and sample preparation. Calibration standards were prepared with internal standards in the following concentration ranges: glutamine and glutamate 0.05–250 μM; lactate 0.05–500 μM; 2-OH-glutarate 0.1–200 μM, all other metabolites 0.05–100 μM. Internal standards were added to 500 μl of cell extract, evaporated with nitrogen and reconstituted in 50 μl of eluent solvent A. UPLC/MS-grade methanol, formate, citrate, isocitrate, fumarate, pyruvate, succinate, lactate, malate, α-ketoglutarate, 2-OH-glutarate, glutamate and glutamine and the internal standards $^{13}C_2$-succinate and $^{13}C_3$-lactate were obtained from Sigma–Aldrich, Denmark. The internal standards $^2H_4$-α-ketoglutarate, $^{13}C_5$, ^{15}N-Glutamate and $^2H_5$_Glutamine were obtained from Cambridge Isotope Laboratories, Inc., USA. Water was provided by a millipore system.

3.3.2.3. Metabolite detection. Detection of the metabolites was performed using a Waters Xevo™ triple quadrupole tandem mass spectrometer (Waters Corp, Manchester, UK) with a *Z*-spray electrospray ionization (ESI) source operating both in the positive and negative ion modes. The mass spectrometer was tuned for each individual metabolite to obtain the maximum intensity for the precursor ions (Table S1). The following parameters were used for ESI-MS analysis in negative ion/positive ion mode: capillary (kV) 2.5/3.0, extractor (V) 3/3, LM1 (low mass)/HM1 (high mass) resolution 3.0/15.0 and LM2/HM2 resolution 3.0/15.0. Desolvation gas at a flow rate of 800 l/h. Desolvation at a temperature of 600 °C. The cone and

collision gas (argon) flows were set to 20/25 l/h and 0.25/0.25 ml/min, respectively. The source temperature remained at 150 °C.

3.3.2.4. Data analysis. Chromatographic data were analyzed with Waters MassLynx v4.1 software. Quantification was achieved for each analyte using linear regression analysis of the peak area ratio analyte/IS (weighed $1/X$) versus concentration. The assay was performed in biological triplicates. The data was corrected for total protein.

Authors contributions

LR, PH, NMVD and JJMJ contributed to the concept and design of the study. JJMJ coordinated the study. LR, MLPR, JG, YFT, AMW, RH and GH contributed to the acquisition and interpretation of the data. LR wrote the manuscript. All co-authors critically revised the manuscript and provided final approval of the manuscript to be published.

Declaration of Competing Interest

The authors declare no conflicts of interest in preparing this article.

Acknowledgments

We thank Fried Zwartkruis and Hanneke Haijes-Siepel (UMC Utrecht) for helpful discussions. This project has not been funded.

Appendix A. Supplementary data

Supplementary data to this article can be found online at https://doi.org/10.1016/j.bbagen.2019.129484.

References

[1] N.P. Curthoys, M. Watford, Regulation of glutaminase activity and glutamine metabolism, Annu. Rev. Nutr. 15 (1995) 133–159.
[2] J.G. Cory, A.H. Cory, Critical roles of glutamine as nitrogen donors in purine and pyrimidine nucleotide synthesis: asparaginase treatment in childhood acute lymphoblastic leukemia, In Vivo 20 (2006) 587–589.
[3] B.J. Altman, Z.E. Stine, C.V. Dang, From Krebs to clinic: glutamine metabolism to cancer therapy, Nat. Rev. Cancer 16 (2016) 619–634.
[4] J. Zhang, N.N. Pavlova, C.B. Thompson, Cancer cell metabolism: the essential role of the nonessential amino acid, glutamine, EMBO J. 36 (2017) 1302–1315.
[5] H.A. Krebs, Metabolism of amino-acids: the synthesis of glutamine from glutamic acid and ammonia, and the enzymic hydrolysis of glutamine in animal tissues, Biochem. J. 29 (1935) 1951–1969.
[6] L. Rumping, F. Tessadori, P.J.W. Pouwels, E. Vringer, J.P. Wijnen, A.A. Bhogal, S.M.C. Savelberg, K.J. Duran, M.J.G. Bakkers, R.J.J. Ramos, et al., GLS hyperactivity causes glutamate excess, infantile cataract and profound developmental delay, Hum. Mol. Genet. 28 (2019) 96–104.
[7] Y. Xiang, Z.E. Stine, J. Xia, Y. Lu, R.S. O'Connor, B.J. Altman, A.L. Hsieh, A.M. Gouw, A.G. Thomas, P. Gao, et al., Targeted inhibition of tumor-specific glutaminase diminishes cell-autonomous tumorigenesis, J. Clin. Invest. 125 (2015) 2293–2306.
[8] X. Xu, Y. Meng, L. Li, P. Xu, J. Wang, Z. Li, J. Bian, Overview of the development of Glutaminase inhibitors: achievements and future directions, J. Med. Chem. (2018), https://doi.org/10.1021/acs.jmedchem.8b00961.
[9] D.M. Miller, S.D. Thomas, A. Islam, D. Muench, K. Sedoris, C-Myc and cancer metabolism, Clin. Cancer Res. 18 (2012) 5546–5553.
[10] V. Nain, R. Buddham, R. Puria, Role of TCA cycle truncation in Cancer cell energetics, Curr. Trends Biotechnol. Pharm. 8 (2014) 428–438.
[11] E. Bayer, B. Bauer, H. Eggerer, Evidence from inhibitor studies for conformational changes of citrate synthase, Eur. J. Biochem. 120 (1981) 155–160.
[12] X.X. Dong, Y. Wang, Z.H. Qin, Molecular mechanisms of excitotoxicity and their relevance to pathogenesis of neurodegenerative diseases, Acta Pharmacol. Sin. 30 (2009) 379–387.
[14] A. Okazaki, P.A. Gameiro, D. Christodoulou, L. Laviollette, M. Schneider, F. Chaves, A. Stemmer-Rachamimov, S.A. Yazinski, R. Lee, G. Stephanopoulos, et al., Glutaminase and poly(ADP-ribose) polymerase inhibitors suppress pyrimidine synthesis and VHL-deficient renal cancers, J. Clin. Invest. 127 (2017) 1631–1645.
[15] S.M. Davidson, T. Papagiannakopoulos, B.A. Olenchock, J.E. Heyman, M.A. Keibler, A. Luengo, M.R. Bauer, A.K. Jha, J.P. O'Brien, K.A. Pierce, et al., Environment impacts the metabolic dependencies of Ras-driven non-small cell lung cancer, Cell Metab. 23 (2016) 517–528.
[16] M. Fumagalli, D. Lecca, M.P. Abbracchio, S. Ceruti, Pathophysiological role of purines and pyrimidines in neurodevelopment: unveiling new pharmacological approaches to congenital brain diseases, Front. Pharmacol. 8 (2017) 941.
[17] D.S. Lynch, V. Chelban, J. Vandrovcova, A. Pittman, N.W. Wood, H. Houlden, GLS loss of function causes autosomal recessive spastic ataxia and optic atrophy, Ann. Clin. Transl. Neurol. 5 (2018) 216–221.
[18] L. Rumping, B. Buttner, O. Maier, H. Rehmann, M. Lequin, J.U. Schlump, B. Schmitt, B. Schiebergen-Bronkhorst, H. Prinsen, M. Losa, et al., Identification of a loss-of-function mutation in the context of glutaminase deficiency and neonatal epileptic encephalopathy, JAMA Neurol. (2018), https://doi.org/10.1001/jamaneurol.2018.2941.
[19] M.I. Gross, S.D. Demo, J.B. Dennison, L. Chen, T. Chernov-Rogan, B. Goyal, J.R. Janes, G.J. Laidig, E.R. Lewis, J. Li, et al., Antitumor activity of the glutaminase inhibitor CB-839 in triple-negative breast cancer, Mol. Cancer Ther. 13 (2014) 890–901.
[20] R.I. Birkler, N.B. Stottrup, S. Hermannson, T.T. Nielsen, N. Gregersen, H.E. Botker, M.F. Andreasen, M. Johannsen, A UPLC-MS/MS application for profiling of intermediary energy metabolites in microdialysis samples – a method for high-throughput, J. Pharm. Biomed. Anal. 53 (2010) 983–990.
[21] M.G.M. de Sain-van der Velden, M. van der Ham, J. Gerrits, H. Prinsen, M. Willemsen, M.L. Pras-Raves, J.J. Jans, N.M. Verhoeven-Duif, Quantification of metabolites in dried blood spots by direct infusion high resolution mass spectrometry, Anal. Chim. Acta 979 (2017) 45–50.
[22] M.C. Chambers, B. Maclean, R. Burke, D. Amodei, D.L. Ruderman, S. Neumann, L. Gatto, B. Fischer, B. Pratt, J. Egertson, et al., A cross-platform toolkit for mass spectrometry and proteomics, Nat. Biotechnol. 30 (2012) 918–920.
[23] C.A. Smith, E.J. Want, G. O'Maille, R. Abagyan, G. Siuzdak, XCMS: processing mass spectrometry data for metabolite profiling using nonlinear peak alignment, matching, and identification, Anal. Chem. 78 (2006) 779–787.
[24] D.S. Wishart, T. Jewison, A.C. Guo, M. Wilson, C. Knox, Y. Liu, Y. Djoumbou, R. Mandal, F. Aziat, E. Dong, et al., HMDB 3.0 – the human metabolome database in 2013, Nucleic Acids Res. 41 (2013) D801–D807.
[25] H.C. Prinsen, B.G. Schiebergen-Bronkhorst, M.W. Roeleveld, J.J. Jans, M.G. de Sain-van der Velden, G. Visser, P.M. van Hasselt, N.M. Verhoeven-Duif, Rapid quantification of underivatized amino acids in plasma by hydrophilic interaction liquid chromatography (HILIC) coupled with tandem mass-spectrometry, J. Inherit. Metab. Dis. 39 (2016) 651–660.
[26] S.M. Robert, H. Sontheimer, Glutamate transporters in the biology of malignant gliomas, Cell. Mol. Life Sci. 71 (10) (2014) 1839–1854.
[27] M.J. Lukey, K.S. Greene, J.W. Erickson, K.F. Wilson, R.A. Cerione, The oncogenic transcription factor c-Jun regulates glutaminase expression and sensitizes cells to glutaminase-targeted therapy, Nat. Commun. 7 (2016) 11321.
[28] M. Zhen, Z. Xian, Y. Jiarong, H. Junjie, H. Jian, T. Yongguang, Sirtuins in metabolism, DNA repair and cancer, J. Exo Clin. Cancer Res. 35 (2016) 182.
[29] L. Faff-Michalak, J. Albrecht, Hyperammonemia and hepatic encephalopathy stimulate rat cerebral synaptic mitochondrial glutamate dehydrogenase activity specifically in the direction of glutamate oxidation, Brain Res. 618 (1993) 299–302.
[30] L. Rumping, J.J.M. Jans, P.M. van Hasselt, Letter to the editor: Glutaminase deficiency caused by short tandem repeat expansion in GLS, N. Engl. J. Med. 381 (2019) 1185.